

Influence of H₂S on the hydrogenation activity of relevant transition metal sulfides

Guernalec Nadège^a, Cseri Tivadar^b, Raybaud Pascal^c,
Geantet Christophe^{a,*}, Vrinat Michel^a

^a*Institut de Recherches sur la Catalyse, 2 Av. A. Einstein, 69626 Villeurbanne Cedex, France*

^b*Institut Français du Pétrole, IFP Lyon, BP3 69390 Vernaison, France*

^c*Institut Français du Pétrole, Division Chimie et Physico-chimie Appliquées, 1-4 Av de Bois-Préau, 92858 Rueil Malmaison, France*

Available online 1 October 2004

Abstract

Volcano curves relationships between hydrodesulfurization (HDS) or hydrogenation (HYD) catalytic activities and the ab initio calculated sulfur–metal bond energy, $E(\text{M–S})$, descriptor of transition metal sulfides (TMS) have been recently established. Such correlations helping to rationalize and predict the design of heterogeneous catalysts can be intuitively understood in the spirit of Sabatier principle. Similar calculations have also revealed the primary importance to better control the influence of the reaction conditions ($P_{\text{H}_2\text{S}}$, P_{H_2} , T) on such periodic trends as well as nature of the active sites. If H₂S is generally considered as an inhibitor of HDS or HYD reactions, the inhibiting effect may depend on the nature of the transition metal sulfide (TMS). The observed HDS or HYD activities may thus be affected by the H₂S partial pressure. The purpose of the present work is to explore the effect of H₂S on the experimental catalytic activities of five relevant γ -alumina supported TMS in toluene hydrogenation. We have undertaken a systematic kinetic study on γ -alumina supported Rh, Ru, NiMo, Mo and Cr sulfides catalysts. Two distinct effects of H₂S are evidenced. Transition metal sulfides with high and intermediate $E(\text{M–S})$ such as Mo, Rh, Ru and NiMo are inhibited by H₂S, whereas the Cr sulfide exhibiting a low $E(\text{M–S})$ reveals an original promoting effect of H₂S.

© 2004 Elsevier B.V. All rights reserved.

Keywords: Transition metal sulfides; Volcano curves; Hydrogen disulfide; Hydrogenation

1. Introduction

Volcano curves derived either from experimental (e.g. nature of the metal versus activity) or theoretical interpretations represent an alternative strategy for the design of new catalytic formulations as compared to trial-and-error experimentation. Such volcano curves have been extensively published for single metal or bimetallic catalysts as well as sulfide catalysts [1,2]. In hydrodesulphurization, these periodic trends have been investigated from both experimental [3] and theoretical sides [4]. From experiments, most of the studies either in HDS, HDN or HYD (hydrogenation of aromatics) on unsupported or supported catalysts agreed with the statement that group VIII metal sulfides of the first row are poorly active whereas second and third rows are

much more active [5–7]. From these experimental observations, many attempts have been proposed for establishing relationships between HDS/HYD activity and intrinsic properties of transition metal sulfides (TMS). For instance, TMS enthalpy of formation [3], the occupation of $2t_{2g}$ levels [8], surface atoms pair potentials [9], the critical points on the valence shell of charge concentration [10,11], bond energy model [12], sulphur addition energy model [13]. However, most of these approaches have failed to correctly render HDS or HYD rate on the large range of TMS. One of the most recent and general approach uses the so called “Yin–Yang” ab initio descriptor [15] enabling the systematic calculation of metal sulphur bond energy in TMS as stable in HDS/HYD reactions [4,14]. Combining such a calculated descriptor with a Langmuir–Hinshelwood model and Brønsted–Evans–Polanyi relationship, a kinetic interpretation of the volcano curves between HDS or HYD rate and the ab initio sulfur bond energies calculated in TMS has

* Corresponding author. Tel.: +33 4 72 44 5336; fax: +33 4 72 44 5399.
E-mail address: geantet@catalyse.univ-lyon1.fr (G. Christophe).

Table 1

Characteristics (metal loading, sulfidation state) of the supported TMS ordered as a function of the “Yin-Yang” sulfur–metal bond descriptor

Catalyst	Metal loading (wt.%)	at/nm ²	S/Me atomic ratio ^a	<i>E</i> (M–S) ^b (kJ/mol)
MoS ₂ /Al ₂ O ₃	10.2	2.7	2.3	166
RuS ₂ /Al ₂ O ₃	5.4	1.3	2.3	141
NiMoS/Al ₂ O ₃	9.3 (Mo) 2.4 (Ni)	2.5 (Mo) 1.1 (Ni)	S/(Ni + Mo): 1.8	128
Rh ₂ S ₃ /Al ₂ O ₃	0.9	0.2	1.3	119
Cr ₂ S ₃ /Al ₂ O ₃	6.6	3.16	1.3	97

^a From S analysis or EDS.^b According to the values of the “Yin-Yang” descriptor as calculated in Ref. [15].

been established [15]. This approach also gave a theoretical interpretation of the synergic effect exhibited by the Co or Ni promoted MoS₂ (or WS₂) catalysts. Furthermore, ab initio studies also revealed the key influence of the H₂/H₂S partial pressures on the nature of promoted active sites [16,17]. As a consequence, one expects from these results that the reaction conditions influence the trends in activity of the TMS catalysts. Up to now, most of the available experimental data often refer to specific experimental conditions, and do not investigate in a consistent way, the effect of H₂S partial pressures on the relative activities for a wide range of TMS. Besides, specific studies focusing on one given catalyst investigate the role of H₂S, and complex reaction mechanisms were proposed according to these results [18,19]. Furthermore, intriguing properties such as 0 orders with respect to H₂S for Nb sulfide catalysts were reported [20].

As a consequence, the purpose of the present paper is to investigate the influence of the H₂S partial pressure on the toluene hydrogenation activity for five “relevant” TMS supported on γ -alumina. We mean by “relevant”, TMS exhibiting “Yin-Yang” descriptor values covering a representative interval of sulfur–metal bond energies as given in ref. [15]. On the low S–M energy region (ascending branch of the volcano), we choose Cr₂S₃, on the high S–M energy region (descending branch) MoS₂. Close to the optimum S–M bond energy (summit of the volcano) the Rh₂S₃ and RuS₂ sulfides is investigated. A comparison with alumina supported NiMoS conventional catalyst is also performed. The different values of S–M bond energies are reported in Table 1 according to ref. [15].

2. Experimental

2.1. Catalysts preparation

A commercial NiMoS on alumina catalyst (9.33 wt.% Mo (2.54 atMo/nm²) and 2.36 wt.% Ni, specific surface area 230 m²/g, and pore volume 0.48 cm³/g) was used as a reference and activated in a 15% H₂S/H₂ flow at 673 K for 4 h. Mo, Ru, Rh and Cr catalysts were prepared by pore-filling impregnation of a γ -Al₂O₃ support (surface area is 240 m²/g, and pore volume is 0.61 cm³/g) with respectively (NH₄)₆Mo₇O₂₄·4H₂O, RuCl₃, [(NH₃)₅Rh]Cl₃ and Cr(NO₃)₃.

The metal salts were dissolved in water. The catalysts were drying over night at room temperature and 10 h at 373 K. Subsequently only Mo and Rh catalysts were calcined respectively at 673 K for 4 h and 523 K for 1 h in a flow of air. After all the catalysts were sulfided: Ru and Rh in a 15% H₂S/N₂ flow at 673 K for 4 h; Mo and Cr in a 15% H₂S/H₂ flow at 673 K for 4 h. It is important during the activation procedure to avoid a too reductive atmosphere in the case of Ru and Rh to obtain the fully sulfided state [21]. Table 1 summarizes the metal loading and sulfidation state of the series of supported catalysts.

Unsupported chromium sulfide was obtained from the direct sulfidation with pure H₂S of anhydrous CrCl₃ at 713 K for 4 h. The specific surface area of the sample after catalytic test is 49 m²/g. Its composition according to chemical analysis (S/Cr atomic ratio of 1.6) and XRD corresponds to a Cr₂S₃ phase.

2.2. Catalytic testing

Hydrogenation (HYD) of toluene is used as a model reaction to determine the catalytic activities of the catalysts. The test was performed under dynamic conditions with various H₂S partial pressures, obtained by dilution of H₂S/H₂ standard mixtures, in the following conditions: $P_{\text{total}} = 3.5 \times 10^3$ kPa, total flow rate = 80 mL/min, $P_{\text{Toluene}} = 5.6$ kPa and $T_{\text{reaction}} = 623$ K. The mass of the catalysts was varied in order to get a conversion below 20%. Specific activity was measured, according to first-order kinetics, after 15 h on stream in the pseudo-stationary state once the steady state is reached. Different relevant levels of H₂S partial pressures were chosen in the range of 0.52–12 kPa. Within our standard procedure, the successive levels of H₂S partial pressures have been chosen in a random manner alternatively between high and low partial pressures. Moreover, a back point was always performed to estimate the catalyst deactivation during time. Except in the case of RuS₂, we noticed a small deactivation of the catalysts during the test.

2.3. Characterizations

Several techniques such as TEM combined with EDS (Jeol 2010), C–S analysis (Juve), XRD (Bruker D5005) and

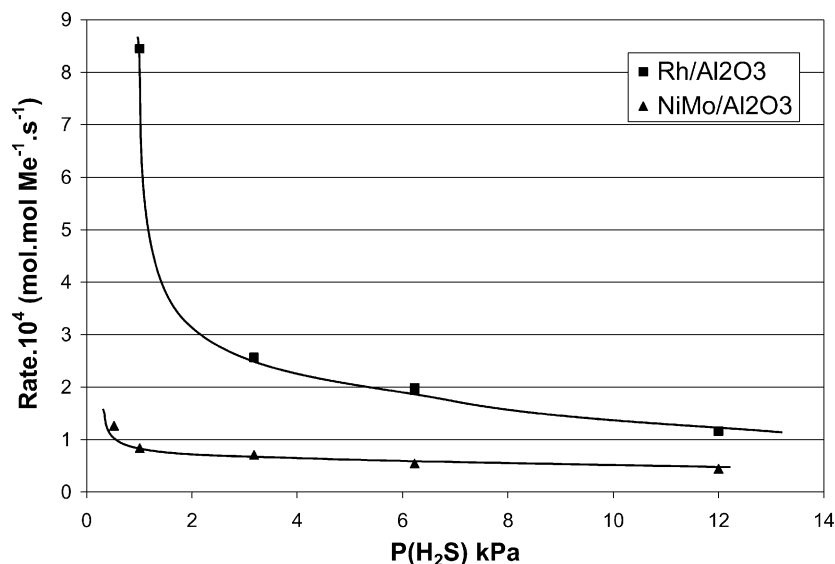


Fig. 1. Effect of H₂S partial pressure on the catalytic conversion of toluene on a Rh₂S₃/Al₂O₃ and NiMoS/Al₂O₃ sulfide catalysts.

chemical analysis were used for the characterization of the catalysts.

3. Results and discussion

Figs. 1–3 illustrate the catalytic behaviour of the series of catalysts. Due to the large variation of catalytic activities, we separate the results in order to compare the catalysts working in the same range of activity. This activity is expressed per metal atom since various atomic loading were used (see Table 1). The reaction temperature used, 623 K, represented the best compromise in order to get measurable catalytic activities for the series of catalysts. As illustrated

in Figs. 1–3, and as expected by the volcano curves established elsewhere [4,14,15], the Mo sulfide (respectively Cr sulfide) catalyst, having the highest (respectively the lowest) S–M bond energy (see Table 1), exhibit the lowest rates. Over the interval of H₂S partial pressures, the Rh sulfide system presents the highest HYD activities. This catalyst is followed by the commercial NiMoS catalyst. It has to be stressed that those two catalysts present intermediate S–M bond energies as shown in Table 1, also in agreement with the volcano relationship.

In order to confirm more quantitatively this trend, we have used a similar kinetic model as proposed in ref. [15]. It is based on a simple Langmuir–Hinshelwood mechanism, with is often used in the case of hydrotreating reactions

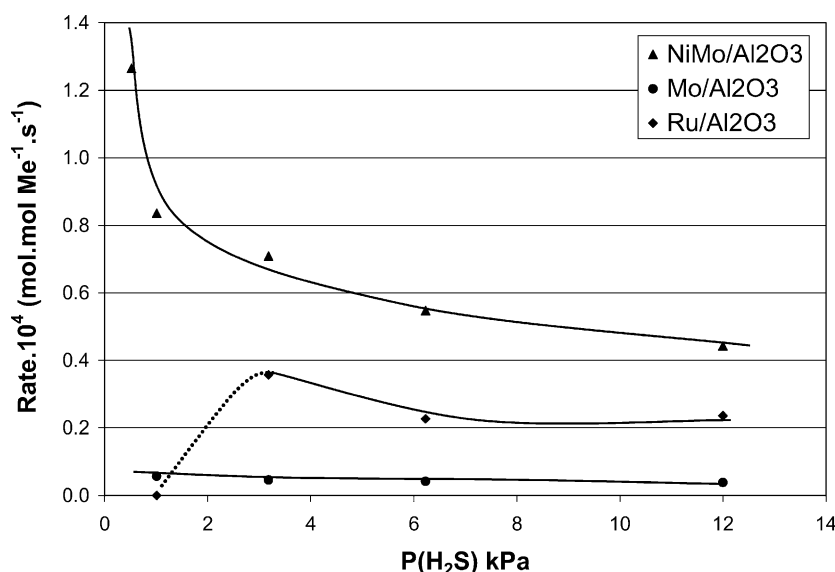


Fig. 2. Effect of H₂S partial pressure on the catalytic conversion of toluene on a RuS₂/Al₂O₃, MoS₂/Al₂O₃ and NiMoS/Al₂O₃ sulfide catalysts.

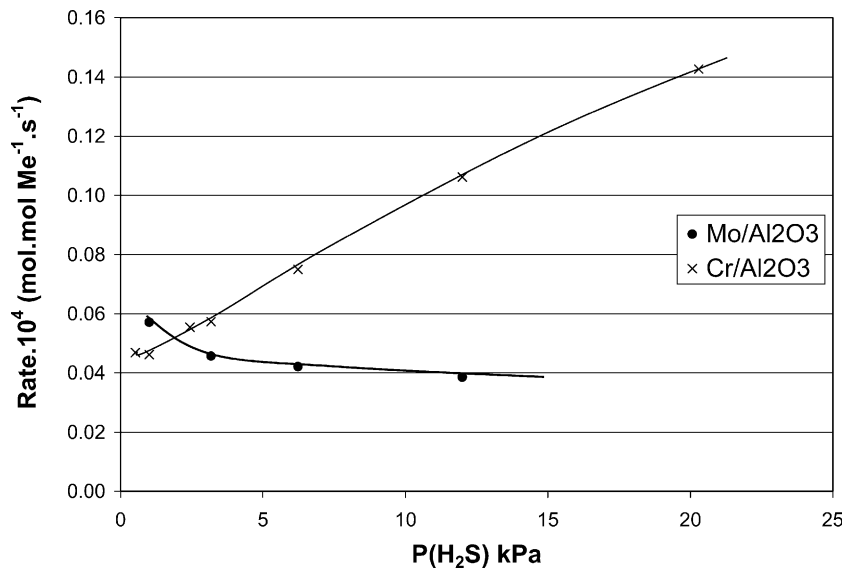


Fig. 3. Effect of H₂S partial pressure on the catalytic conversion of toluene on a MoS₂/Al₂O₃ and Cr₂S₃/Al₂O₃ sulfide catalysts.

[22,23], involving a bimolecular rate determining step in the adsorbed phase:



where A stands for toluene, B for H₂, and C for the hydrogenated species desorbing rapidly from the surface. Because H₂S is introduced in the reaction conditions, it will adsorb simultaneously on the catalyst, assuming it compete for the same single site as toluene and H₂. We thus obtain the following Langmuir rate equation, for a given catalyst of type *j*:

$$r_j = \left(\frac{kT}{h} \right) P_{\text{Tol}} P_{\text{H}_2} \exp \left(\frac{-\Delta G_j^\pm - \Delta G_{j,\text{Tol}}^{0,\text{ads}} - \Delta G_{j,\text{H}_2}^{0,\text{ads}}}{RT} \right) \times \left[1 + P_{\text{Tol}} \exp \left(\frac{-\Delta G_{j,\text{Tol}}^{0,\text{ads}}}{RT} \right) + P_{\text{H}_2} \exp \left(\frac{-\Delta G_{j,\text{H}_2}^{0,\text{ads}}}{RT} \right) + P_{\text{H}_2\text{S}} \exp \left(\frac{-\Delta G_{j,\text{H}_2\text{S}}^{0,\text{ads}}}{RT} \right) \right]^{-2} \quad (2)$$

where ΔG_j^\pm stands for the true activation free enthalpy of reaction (1) for the catalyst *j*, and $\Delta G_{j,i}^{0,\text{ads}}$ for the adsorption free enthalpy energy of species *i* = toluene, H₂ or H₂S on catalyst *j*. For the present work, we assume that there is no variation of ΔG_j^\pm with the type of catalyst *j* (the coefficient of Brønsted–Evans–Polanyi relationship is equal to zero). Besides, we use similar linear relationship between $\Delta G_{j,i}^{0,\text{ads}}$ and the sulfur–metal bond energy as already proposed in ref. [15]:

$$\Delta G_{j,i}^{0,\text{ads}} = \beta_i E_j + \Delta G_{0,i}^{0,\text{ads}} \quad (3)$$

where $E_j = E(\text{M–S})$ calculated for the bulk phase of the sulfide catalyst, *j*.

Within this framework, the expression of the rate depends on one single variable, i.e. the ab initio calculated $E(\text{M–S})$. Using the present experimental data, as reported in Figs. 1–3, we obtain the volcanoes as drawn in Fig. 5 (the fitting parameters, β_j , are given in the figure's caption). At this stage, it must be stressed that the fit of the kinetic modeling might certainly be improved in the future, thanks to complementary

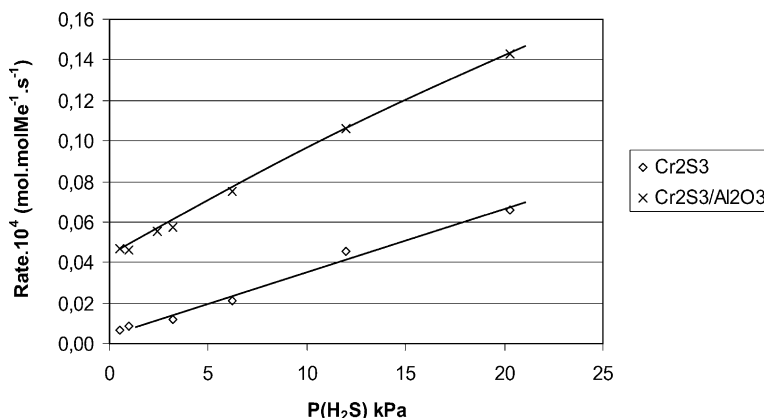


Fig. 4. Effect of H₂S partial pressure on the catalytic conversion of toluene on a Cr₂S₃/Al₂O₃ and Cr₂S₃ sulfide catalysts.

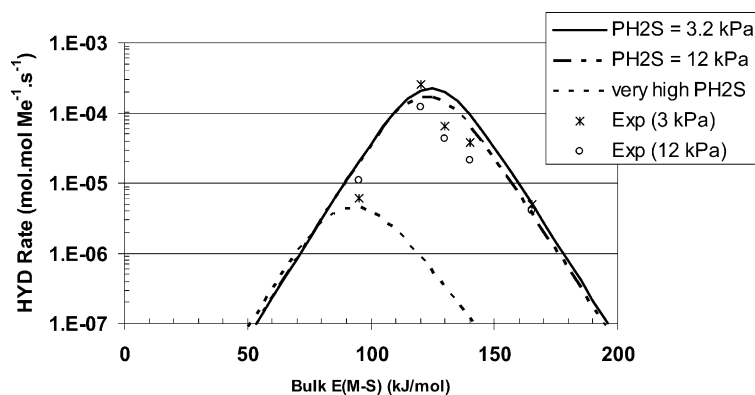


Fig. 5. Rate of toluene hydrogenation as a function of the bulk sulfur–metal bond energy as defined in ref. [15] and for different $P(\text{H}_2\text{S})$. The fitting parameters are $\beta(\text{Toluene}) = 0.67$ and $\beta(\text{H}_2\text{S}) = 0.60$. For H_2 , we assume as in ref. [15] that the adsorption free enthalpy is the same for all catalysts.

(theoretical or experimental) data on activation energies or adsorption energies over a wider range of TMS.

Concerning the H_2S effect, our experimental results show that alumina supported Rh_2S_3 is much more sensitive to H_2S than the NiMoS catalyst. The determination of the kinetic orders with respect to hydrogen sulfide obtained from \ln – \ln plots is reported in Table 2. Finally, it can be resumed that the inhibiting effect of H_2S varies in the following order $\text{Mo} < \text{NiMo} < \text{Ru} < \text{Rh}$. In the case of RuS_2 , it must be stressed that a kinetic order in H_2S equal to -0.67 is found at high partial pressure ($3.18 \text{ kPa} < P(\text{H}_2\text{S}) < 12 \text{ kPa}$). However, at low H_2S partial pressure, the catalytic activity irreversibly drops down to zero, indicating a strong structural modification of the catalysts. This behaviour is attributed to the thermodynamic stability of the nanoparticles of RuS_2 . According to TEM measurements, average particle size is close to 25 \AA . Under our catalytic conditions (623 K , high hydrogen partial pressure), and according to TPR-like experiments such particles are considerably reduced [24,25], and we can expect that the RuS_2 structure collapses. The S/Ru atomic ratio determined after catalytic testing under these reducible conditions is 0.3 . Since no intermediate phase exists in the Ru–S phase diagram, we can assume that the catalyst is now composed of Ru metallic particles mainly poisoned by sulfur on its surface. It has been checked that on unsupported RuS_2 with larger particle sizes such a deactivation is not observed in the same domain of low partial pressure. So, the stability of the supported RuS_2

phases drastically depends on the RuS_2 particles sizes and the $P_{\text{H}_2\text{S}}/P_{\text{H}_2}$ ratio.

Chromium sulfide supported catalysts exhibit a completely new behaviour since a positive effect of H_2S is observed. As illustrated in Fig. 3, the conversion rate increases linearly with H_2S content in the feed. In fact, this catalyst gives a more complex reaction scheme than the simple toluene into methylcyclohexane conversion observed for the other TMS catalysts. Isomerised and cracked products such as 2,3-dimethylpentane, dimethylcyclopentanes and ethylcyclopentane are obtained. However, conversions into all different types of products are increased with higher H_2S partial pressure. A similar study performed on unsupported Cr_2S_3 catalysts confirmed that this is an intrinsic property of this TMS (see Fig. 4). The phenomenon is reversible which illustrates the stability of the Cr_2S_3 active phase in the investigated range of H_2S partial pressure (0.5 – 20 kPa).

Using the previously defined Langmuir–Hinshelwood formalism, we are able to explore the effect of $P(\text{H}_2\text{S})$, and thus to determine the ratio of the constant $K_T/K_{\text{H}_2\text{S}}$ as well as K_T/K_{H_2} . The values are reported in Table 2 for the different catalysts as a function of $E(\text{M-S})$. These values show that the $K_T/K_{\text{H}_2\text{S}}$ ratio varies in small range as a function of the catalyst. Both species (toluene and H_2S) may thus compete for the adsorption on the site, even if toluene adsorption appears as being slightly more favoured. Moreover, we notice that the ratio increases with $E(\text{M-S})$ meaning that

Table 2

Ratio of the adsorption constant as given by the Langmuir–Hinshelwood model and apparent order (experimentally determined) for H_2S for the different TMS/ Al_2O_3 catalysts

Catalyst	$K_T/K_{\text{H}_2\text{S}}$	K_T/K_{H_2}	$E(\text{M-S})$ (kJ/mol)	Apparent order n (H_2S)
$\text{MoS}_2/\text{Al}_2\text{O}_3$	8.7	1.1×10^5	166	-0.15
$\text{RuS}_2/\text{Al}_2\text{O}_3$	6.3	4.3×10^3	141	-0.67^a
$\text{NiMoS}/\text{Al}_2\text{O}_3$	5.5	1.2×10^3	128	-0.34
$\text{Rh}_2\text{S}_3/\text{Al}_2\text{O}_3$	4.8	326	119	-0.84
$\text{Cr}_2\text{S}_3/\text{Al}_2\text{O}_3$	3.5	13	97	$+0.47^b$

^a Calculated on the range of $P(\text{H}_2\text{S})$ 3.18–12 kPa.

^b Calculated on the range of $P(\text{H}_2\text{S})$ 3.18–20.3 kPa for methylcyclohexane formation.

toluene is adsorbed even more strongly in the region of large values of $E(M-S)$. For H_2 , we observe that it is far less strongly adsorbed than toluene (or H_2S). The volcano's region where H_2 is favoured is for small $E(M-S)$ values, where many S-vacancies are available. Since toluene is simultaneously less adsorbed on the surface for low $E(M-S)$, the hydrogenation rate drops, explaining the volcano shape of the correlation. Upon increase of $P(H_2S)$ up to 12 kPa, Fig. 5 shows that the hydrogenation rate decreases as observed experimentally for Rh, NiMo, Ru, and Mo sulfides catalysts. Moreover, the decrease in HYD rate is even higher close to the maximum of the volcano (for Rh_2S_3 as observed experimentally). For MoS_2 exhibiting high S–M bond energy, the rate is less affected, as it is also observed. In the low S–M energy region, the behaviour of Cr_2S_3 is more peculiar. The kinetic modelling reveals that this volcano region is even less sensitive to H_2S pressure than the remaining part of the curve. For instance, for $P(H_2S)$ close to the experimentally tested value, we notice that the HYD rate of Cr_2S_3 remains almost constant. We virtually increase $P(H_2S)$ at high values (see Fig. 5) confirming this trend, and observe a slight enhancement of the hydrogenation rate for very low $E(M-S)$. At this stage, we cannot exclude that the HYD rate enhancement induced by H_2S , might be better rendered by the kinetic modelling using improved fittings. As a consequence, to clarify the peculiar promoting effect of H_2S on Cr_2S_3 , we need further investigations. On the one hand, complementary experimental data are required to better understand the mechanism on Cr sulfides. On the other hand, more complex kinetic models might be eventually tested as already proposed for toluene hydrogenation [19] and DBT HDS [18].

4. Conclusion

The present study reveals the effect of H_2S on the toluene HYD of five relevant transition metal sulfides. We have confirmed, as already established in previous study [15], that a Langmuir–Hinshelwood kinetic modeling combined with the $E(M-S)$ descriptor captures the general trend of the toluene hydrogenation rate. In particular, volcano shape relationship is obtained for the five TMS tested. The effect of $P(H_2S)$ for transition metal sulfides located on the summit and descending branch of the volcano curve is well rendered by the kinetic modeling. The stronger decrease of the HYD rate close to the maximum (for Rh sulfides) and the smaller decrease for high $E(M-S)$ for low $P(H_2S)$ have been modelled. The more subtle H_2S promoting effect observed experimentally for Cr sulfide based catalysts remains to be

more carefully investigated. As the reaction involves hydrogenating sites together with acidic sites, we propose in forthcoming works to further investigate this catalyst both from an experimental point of view, and from more complex kinetic modeling.

Acknowledgement

The authors would like to be grateful to Hervé Toulhoat at IFP for fruitful discussions.

References

- [1] R.I. Masel, Principles of Adsorption and Reaction on Solid Surfaces, Wiley Interscience, New York, 1996.
- [2] J.B. Moffat, Theoretical Aspects of Heterogeneous Catalysis, Van Nostrand Reinhold Catalysis Series, New York, 1990.
- [3] T.A. Pecoraro, R.R. Chianelli, J. Catal. 67 (1981) 430.
- [4] H. Toulhoat, P. Raybaud, S. Kasztelan, G. Kresse, J. Hafner, Catal. Today 50 (1999) 629.
- [5] M. Lacroix, N. Boutarfa, C. Guillard, M. Vrinat, M. Breyse, J. Catal. (1989) 473.
- [6] J.P.R. Vissers, C.K. Groot, E.M. Van Oers, V.H.J. De Beer, R. Prins, Bull. Soc. Chim. Belg. 93 (1984) 813.
- [7] M.J. Ledoux, O. Michaux, G. Agostini, J. Catal. 102 (1986) 275.
- [8] A. Tan, S. Harris, Inorg. Chem. 37 (1998) 2215.
- [9] J.K. Burdett, J.T. Chung, Surf. Sci. Lett. 236 (1990) 353.
- [10] Y. Aray, J. Rodriguez, D. Vega, E.N. Rodriguez-Arias, Angew. Chem. Int. Ed. 39 (2000) 3810.
- [11] Y. Aray, J. Rodriguez, Chem. Phys. Chem. 10 (2001) 599.
- [12] J.K. Nørskov, B.S. Clausen, H. Topsøe, Catal. Lett. 13 (1992) 1.
- [13] E.J.M. Hensen, H.J.A. Brans, G.M.H.J. Lardinois, V.H.J. De Beer, J.A.R. Van Veen, R.A. Van Santen, J. Catal. 192 (2000) 98.
- [14] R.R. Chianelli, G. Berhault, P. Raybaud, S. Kasztelan, J. Hafner, H. Toulhoat, Appl. Catal. 227 (2002) 83.
- [15] H. Toulhoat, P. Raybaud, J. Catal. 216 (2003) 63.
- [16] P. Raybaud, J. Hafner, G. Kresse, S. Kasztelan, H. Toulhoat, J. Catal. 189 (2000) 129; P. Raybaud, J. Hafner, G. Kresse, S. Kasztelan, H. Toulhoat, J. Catal. 190 (2000) 128.
- [17] H. Schweiger, P. Raybaud, H. Toulhoat, J. Catal. 212 (2002) 33.
- [18] E. Olguin Orozco, M. Vrinat, Appl. Catal. A: Gen. 170 (1998) 195.
- [19] S. Kasztelan, D. Guillaume, Ind. Eng. Chem. Res. 33 (1994) 203.
- [20] V. Gaborit, N. Allali, M. Danot, C. Geantet, M. Cattenot, M. Breyse, F. Diehl, Catal. Today 2857 (2002) 1.
- [21] J.A. de Los Reyes, S. Göbölös, M. Vrinat, M. Breyse, Catal. Lett. 5 (1990) 17.
- [22] M.L. Vrinat, Appl. Catal. 6 (1983) 137.
- [23] T. Kabe, A. Ishihara, W. Qian, Hydrodesulfurization and Hydrodenitrogenation, Wiley-VCH, Weinheim, 1999, p. 31.
- [24] J.A. de Los Reyes, M. Vrinat, C. Geantet, M. Breyse, Catal. Today 10 (1991) 645.
- [25] G. Berhault, M. Lacroix, M. Breyse, F. Maugé, J.C. Lavalley, L. Qu, J. Catal. 170 (1997) 37.